

Article

Not peer-reviewed version

Calcination-Enhanced Laser Induced Damage Threshold of 3D Micro-Optics Made with Laser Multi-Photon Lithography

[Darius Gailevičius](#) , Rokas Zvirblis , [Karolis Galvanauskas](#) , Gintare Bataviciute , [Mangirdas Malinauskas](#) *

Posted Date: 27 April 2023

doi: 10.20944/preprints202304.1052.v1

Keywords: LIDT; Laser-Induced Damage Threshold; 3D Micro-optics; Laser Direct Writing; Multi-Photon Lithography; SZ2080™; Calcination; Thermal Treatment; Polymers; Glass





Preprints.org is a free multidiscipline platform providing preprint service that is dedicated to making early versions of research outputs permanently available and citable. Preprints posted at Preprints.org appear in Web of Science, Crossref, Google Scholar, Scilit, Europe PMC.

Copyright: This is an open access article distributed under the Creative Commons Attribution License which permits unrestricted use, distribution, and reproduction in any medium, provided the original work is properly cited.

Article

Calcination-Enhanced Laser Induced Damage Threshold of 3D Micro-Optics Made with Laser Multi-Photon Lithography

Darius Gailevicius , Rokas Zvirblis, Karolis Galvanauskas, Gintare Bataviciute and Mangirdas Malinauskas * 

Current address: Laser Research Center, Vilnius University, Sauletekio Av. 10, LT-10223 Vilnius, Lithuania

* Correspondence: mangirdas.malinauskas@ff.vu.lt;

Abstract: Laser Direct Writing (LDW), also known as 3D multi-photon laser lithography of resins, is a promising technique for fabricating complex free-form elements, including micro-optical functional components. Regular organic or hybrid (organic-inorganic) resins are often used, with latter exhibiting better optical characteristics, as well as having the option to be heat-treated into inorganic glass-like structures, particularly useful for resilient micro-optics. While this work is a continuation of SZ2080™ calcination development [1], the Laser-Induced Damage Threshold (LIDT) of such sol-gel-derived glass micro-structures, particularly those that undergo heat treatment, has not been well-characterized. In this pilot study, we investigated the LIDT using the Series-on-One (S-on-1) protocol of functional micro-lenses produced via LDW and subsequently calcinated. Our results demonstrate that the LIDT can be significantly increased, even multiple times, by this approach, thus enhancing the resilience and usefulness of these free-form micro-optics. This work represents the first investigation in terms of LIDT into the impact of calcination on LDW produced sol-gel-derived glass micro-structures, and provides important insights for the development of robust micro-optical devices.

Keywords: LIDT; Laser-Induced Damage Threshold; 3D Micro-optics; Laser Direct Writing; Multi-Photon Lithography; SZ2080™; Calcination; Thermal Treatment; Polymers; Glass

1. Introduction

The field of laser multi-photon lithography is witnessing rapid progress [2], with an increasing number of micro-optical devices [?] being produced at the micro-scale. These devices include conventional [3] and Fresnel micro-lenses [4], holographic elements [5], polarisation controlled lens arrays [6], meta-optics [7] and multi-component systems [8], most notably, micro objectives [9], non-linear excitation imaging systems [10], as well as anti-reflective coated complex systems [11]. Furthermore, grayscale lithography was utilized to create step-free micro-lens systems either by using increased resolution [12] or variable laser fluence [13]. LDW method may also be used as an alternative for "classic" lithography, especially flexible maskless diffractive imaging systems [14]. Furthermore, precise systems such as microfluidic devices with complex geometries and high aspect ratios [15] as well as actively tuneable photonic crystals with sub-micron features [16] also benefit from LDW.

Distinct benefits of the LDW method are <200 nm resolution [17], ease of manufacturing compared to traditional methods in micro- and nano-scale, the vast availability of organic and hybrid resins, various post-processing steps, such as optical coating deposition [11] and calcination into inorganic glass [18–20]. However, one problem that has been often overlooked with micro-optics produced by LDW is their laser-induced damage threshold (LIDT) behavior. This can pose a significant limitation for applications that involve modern high-intensity pico- and femtosecond pulses since high LIDT is not always guaranteed.

Classical measurement of LIDT for coating (thin film) and bulk objects is standardized [21] and industrially beneficial, however, it is rarely utilized for LDW fabricated elements. Several attempts have been made to measure such element LIDT, and the results have shown variations based on

various factors, such as the resin type used (organic or hybrid) [22–24], the presence of a photo-initiator (PI) [25], and the type of structure produced, whether it is a thin-film [24] or bulk object [26] or a free-form device [27,28]. While some methods can increase LIDT, such as using resins without PI [29] or a less organic composition [30], we propose an alternative approach. We aim to create purely inorganic structures using a heat-based post-processing method (calcination) while retaining the benefits of the LDW method [31].

For hybrid prepolymers such as SZ2080™ [32], calcination above 1000 °C results in an inorganic composite glass or glass-ceramic phase while retaining the printed geometry with homogeneous and repeatable shrinking [1]. It is often assumed that transparent glassy structures should feature higher LIDT values and, therefore, must be more resilient to high-intensity radiation, but this idea has not been tested before [27]. However highly mechanically resilient silicon oxycarbide structures have already been fabricated by utilizing calcination [33].

In this paper, we aim to fabricate suspended and functional structures-micro-lenses, heat-treat them, and confirm the useful increase in LIDT. Figure 1 illustrates the process and the resulting structures.

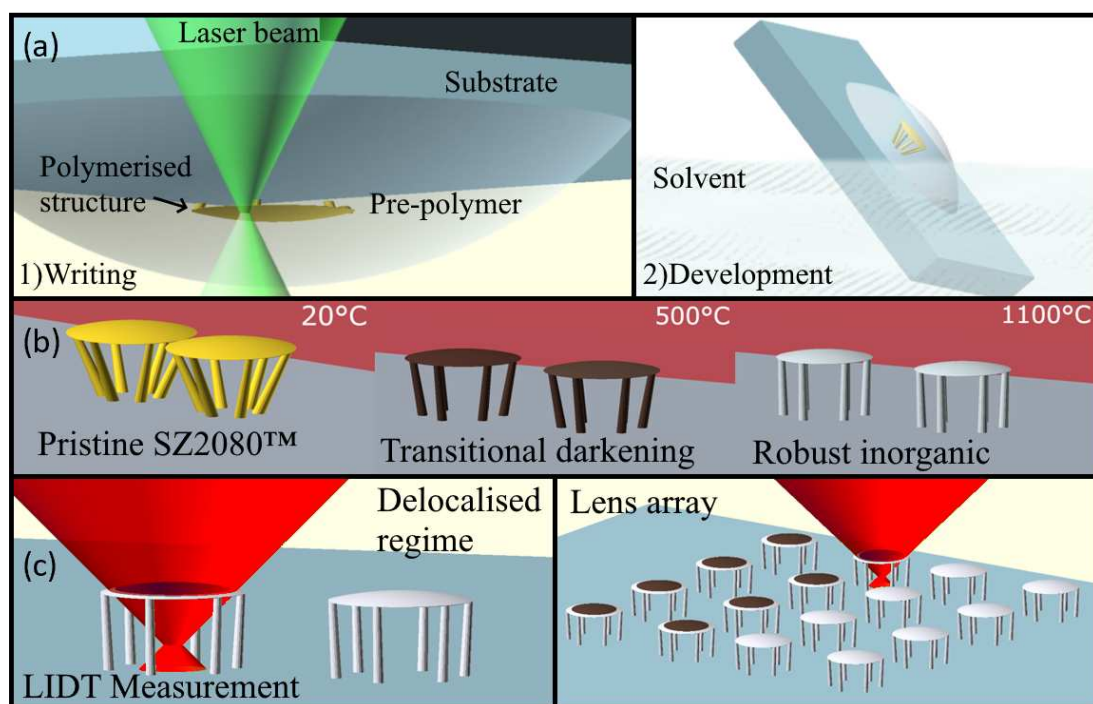


Figure 1. The experimental principle. (a) the fabrication of the test lens structure in resin, (b) heat treatment of the structure and compliant columns, (c) the exposure of the structures to measure the LIDT values.

2. Fabrication

To produce the lenses, we used the low-shrinkage organic-inorganic prepolymer SZ2080™ [34]. The preparation and exposure conditions (Figure 1a) were selected following the methodology reported in [34], using a 63x 1.4 NA Plan-Apochromat immersion oil objective (Zeiss), 517 ± 10 nm wavelength, and 144 fs pulse duration with a repetition rate of 76 MHz. Scanning speed was set to 2000 $\mu\text{m/s}$, while utilizing the Aerotech IFOV technology; beam intensity $\sim 0.4 \text{ TW/cm}^2$. Development was done in Methyl isobutyl ketone for 15 min. The lenses were printed on a quartz substrate, with the final baseline geometry being a plano-convex, 50 μm diameter, 300 μm focal length lens, and a thickness of approximately 2 μm . To support the lenses above the quartz substrate, pillars were printed with an inclination angle of 35° [1] and a total height close to 30 μm . Heat treatment was performed at 1100 °C with a rise time of 12 h and held for 3 h. Transitional reactions with the ambient

atmosphere and carbon-induced darkening are expected at around 500-600°C; however, the final transparent phase generated at the highest treatment temperature is crucial here (Figure 1b overviews the calcination transition).

3. LIDT Metrology

Non-Calcinated (NCA) and Calcinated (CA) samples were qualitatively examined and exposed to the probe beam in damage tests in an array form (Figure 1c). Qualitative characterization of their imaging function was performed in a bright-field microscope to confirm their imaging function before and after LIDT measurements. See Figure 2a for the illustrated concept. The imaging function was used to confirm the occurrence of significant and catastrophic damage events (Figure 2b–e). After, they were characterized using a Scanning Electron Microscope (Model Hitachi TM1000 SEM, Figure 3).

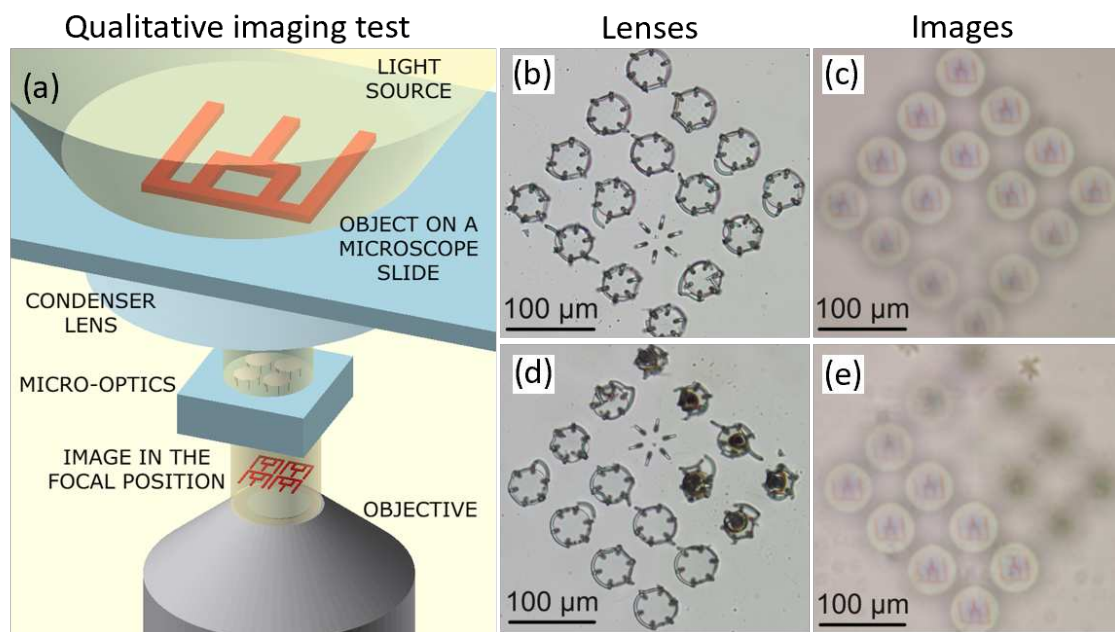


Figure 2. Optical characterization of micro-optics using an inverted microscope: (a) image of the surface of the optic components, (b) an image of the focal position (300 μm) of the same micro-optics, (c) bright-field image after LIDT testing, (d) degradation in image quality in the focal position of damaged lenses, (e) bright-field image after calcination and LIDT testing.

Tests were performed on arrays of micro-lenses. Arrays, mainly composed of 16 lenses, were divided in half to account for damage experiments for NCA (control) and CA (test) micro-optics. Tests were performed in the following sequence: an array of lenses was printed, half of the lenses were exposed before calcination, then the array was calcinated as described previously, and finally, the second half of the lenses was exposed. Laser system parameters used for all experiments were: wavelength $\lambda_1 = 1030 \text{ nm}$ and $\lambda_2 = 515 \text{ nm}$, repetition rate $f = 200 \text{ kHz}$, pulse duration $\tau = 300 \text{ fs}$, Plan-Apochromat Zeiss 20x objective (0.8 NA). S-on-1 damage tests [21] were performed with both wavelengths, exposing the lenses for 50 ms and 5 s, corresponding to 10 000-on-1 and 1 000 000-on-1 pulses.

S-on-1 testing was applied in two regimes (represented in Figure 3f), by varying the applied beam diameter. The first regime is referred to as a local-damage protocol, where the beam diameter is around $4 \mu\text{m}$ ($1/e^2$ intensity level) on the sample. The second regime is referred to as delocalized, where the probe beam diameter is $20 \mu\text{m}$, attained by shifting the (relative to the lens) focus position of the laser beam. The delocalized regime was used to demonstrate the expected behavior where the full aperture of the lens is used, such as in high intensity focusing, while the local regime shows the behavior of a highly focused laser beam on the optics themselves.

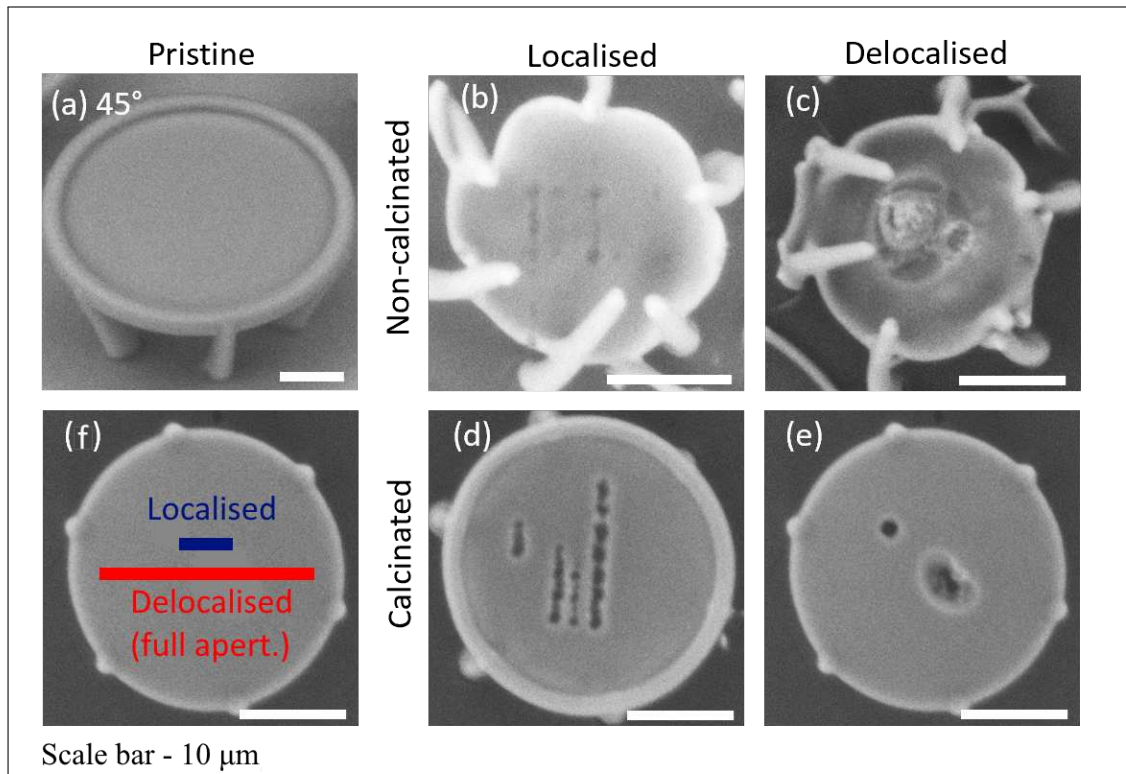


Figure 3. SEM micrographs of micro-lenses, illustrating the typical damage morphologies observed. (a) image of a pristine (untested) NCA lens, (b) local damage regime-tested lens before CA, (c) delocalized damage regime-tested lens before CA, (d) local regime-tested lens after CA, (e) delocalized regime-tested lens after CA, (f) localised and delocalised regime laser spot diameter representation. Tracks are formed around the damage sites for easier visualization.

4. Results

4.1. Morphology

The morphology of the observed damage is depicted in Figure 3. It shows an example of a pristine lens with a diameter of 50 μm that shrinks to 30 μm (40% shrinkage, expected and matching [1]) after calcination (Figure 3a). The localized damage regime results in small ($<1\ \mu\text{m}$) damage sites, while the delocalized-damage regime produces large (approx. 10 μm) damage sites for NCA lenses (Figure 2b). The latter results in catastrophic damage, as most of the aperture becomes distorted and the lenses lose their imaging function. However, CA lenses, as shown in Figure 3d,e, retain their imaging function and exhibit small-diameter ablation sites similar to those produced by fs-laser surface ablation [35]. The morphology does not vary significantly depending on the wavelength used. The only observed difference for NCA lenses is the prominent brown discoloration, particularly for $\lambda = 1030\ \text{nm}$. Previous research by Jonusauskas et al. [36] had concluded that the damage mode of non-calcinated SZ2080TM structures in femtosecond regime is volume heat accumulation. By its nature, SZ2080TM should have a similar heat conductance to other hybrid polymers such as PDMS ([37], 0.2 W/m²K) or Ormocomp (0.4 W/m²K estimated from [38]). It was suggested that better heat load mitigation might increase LIDT. Butkute et al. [27] explained the phenomena as Coulomb explosion-driven dielectric breakdown. In both cases, calcinated Si-Zr glass micro-structures excel in LIDT, by potentially having better heat transfer characteristics (SiO₂-ZrO₂ composites [39] 1 to 3 W/m²K). Also, the minimum bond energy for Si-O (89 kcal/mol) bond in glass is higher than for C-C (80 kcal/mol) or C-O (79 kcal/mol) bonds that constitute the weaker link [40].

4.2. LIDT values

The Figure 4 presents results of LIDT measurements, which include a combination of localized and non-localized damage regimes for NCA and CA lenses, as well as exposure to 10^4 -on-1 and 10^6 -on-1 pulses at 515 and 1030 nm wavelengths. The LIDT values for NCA localized damage regimes were consistent with previously reported scientific data, with $F_{1030} = 0.57 \text{ J/cm}^2$ and $F_{515} = 0.13 \text{ J/cm}^2$ [24,25,30].

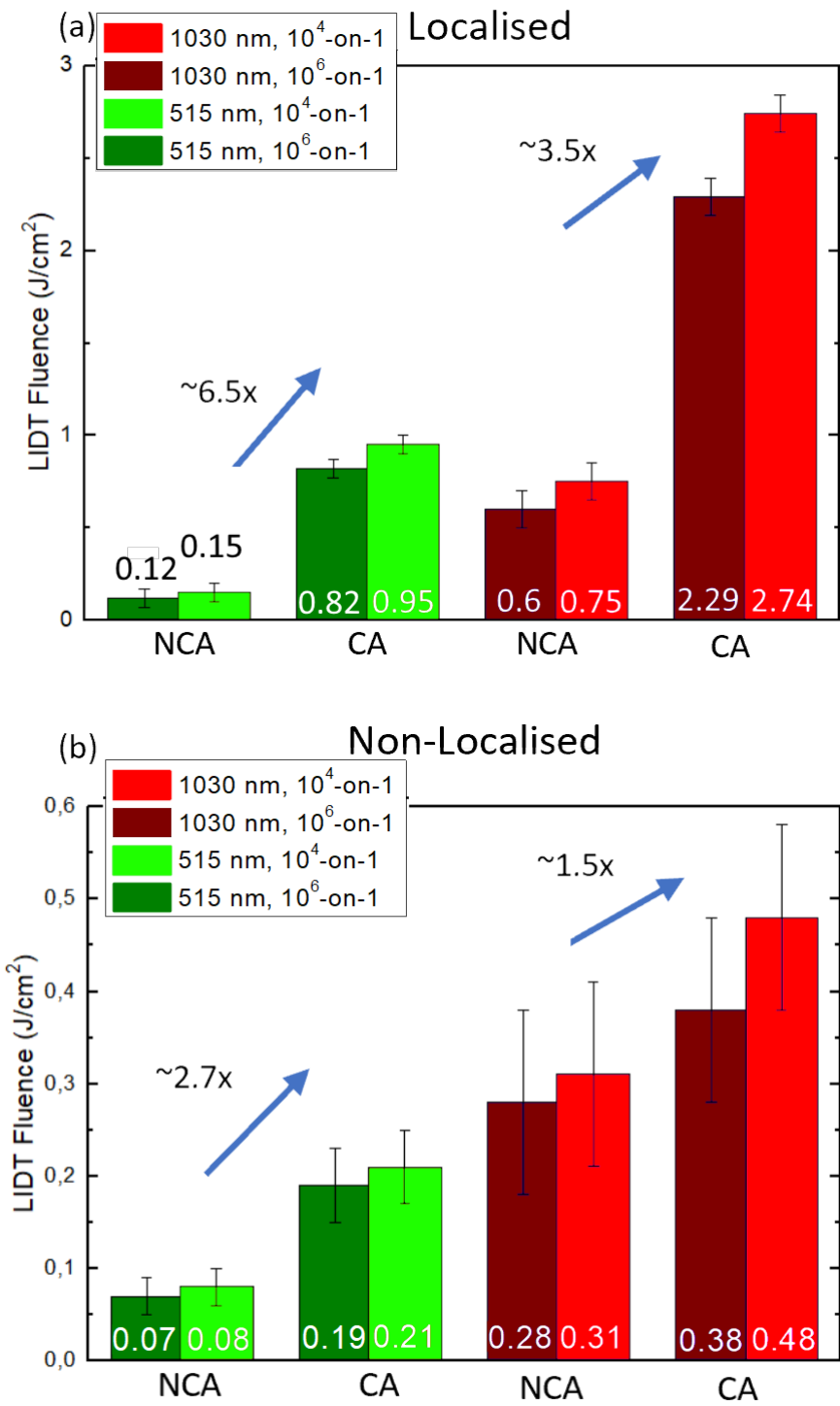


Figure 4. Damage threshold measurement results for (a) localized damage protocol, (b) non-localized damage protocol.

However, the LIDT measured using the non-localized regime is lower compared to known reported values [24,25,30]. It is important to note, however, that the previous experiments using S-on-1 damage testing protocols only exposed the samples to up to 1000 pulses, this could explain the observed differences in measured LIDT values. The current experiments reveal the LIDT degradation in time. Thus, offering a novel insight into calcinated hybrid polymer fatigue behavior.

The results show that local regime LIDT values in calcinated micro-optics exhibit the highest increase. Using a 300 fs laser pulse duration at 1030 nm, a 3-fold increase in laser-induced damage threshold was observed, from $F = 0.6 - 0.8 \text{ J/cm}^2$ to $F = 2.3 - 2.7 \text{ J/cm}^2$. This increase was the highest among all measured values and was consistent across the entire exposure duration range from 50 ms to 5 s. The use of a second harmonic (515 nm) resulted in the highest percentile increase in measured LIDT, with a 6-fold increase in LIDT observed across all exposure durations, from $F = 0.12 - 0.17 \text{ J/cm}^2$ to $F = 0.8 - 0.9 \text{ J/cm}^2$.

However, when exposing in delocalised regime, with an increased exposure area on the CA lens compared to NCA counterparts, a decrease in measured damage thresholds is observed. For the 1030 nm wavelength, the effect of calcination was less pronounced, with only a 1.5 times increase in LIDT observed from $F = 0.28 - 0.31 \text{ J/cm}^2$ for NCA to $F = 0.38 - 0.47 \text{ J/cm}^2$ for calcinated lenses, while 515 nm wavelength exhibited 2.7 times increase in LIDT - from $F = 0.07 - 0.08 \text{ J/cm}^2$ for NCA to $F = 0.19 - 0.21 \text{ J/cm}^2$ for CA lenses.

Overall, results demonstrate that the LIDT values consistently increase for CA micro-lenses, regardless of irradiation area or testing process.

5. Discussion

In this study, we have reported laser-induced damage threshold measurements of SZ2080™ material after calcination for the first time. Our findings demonstrate a significant increase in damage threshold, reaching 3-6 times as a conservative estimate, which supersedes all measured values before [24,25,30]. The maximum measured LIDT value at $\lambda = 1030 \text{ nm}$ is $F = 2.74 \text{ J/cm}^2$, which is relatively large and approaches the level of fused silica [26] $F = 3.11 \text{ J/cm}^2$. These results are promising, as they suggest that the LDW method combined with heat treatment can offer a technologically viable pathway to producing optical-grade glass-level performance micro-optical elements for use in harsh environments in visible and IR wavelengths, as previously postulated.

As this pilot study covers only femtosecond LIDT, further research is needed for other significant regimes, such as the nanosecond and continuous-wave damage tests. In summary, our findings contribute to the field by providing new insights into the performance of SZ2080™ material after calcination and offer exciting possibilities for the development of high-performance micro-optical elements. Furthermore, increased LIDT usually results in increased optics useful lifetime, particularly useful in femtosecond applications [41]. Finally, increased fluence pump sources may be utilized in Glass-on-Glass [42] LDW fabricated micro-lasers, consisting of high-resilience polymers [43].

6. Conclusions

The use of LDW in conjunction with the calcination process for the production of highly resilient micro-optics leads to the following conclusions:

1. LDW fabrication method and SZ2080™ prepolymer without PI allows for the fabrication of sub-100 μm scale micro-lenses with a prospect of calcination [at $T=1100^\circ$], which results in homogeneous shrinkage and glass-like final structures, with no observable darkening, melting, collapse or other functional damage.
2. Calcination of polymerised structures resulted in femtosecond S-on-1 protocol LIDT increase, namely:

(a) Localised regime (beam diameter 4 μm): 3.5x increase in LIDT for 300 fs 1030 nm radiation (from $F = 0.6 - 0.8 \text{ J/cm}^2$ to $F = 2.3 - 2.7 \text{ J/cm}^2$) and 6.5x increase for 515 nm radiation (from $F = 0.12 - 0.17 \text{ J/cm}^2$ to $F = 0.8 - 0.9 \text{ J/cm}^2$) observed across all exposure durations;

(b) Delocalised regime (beam diameter 20 μm -full lens aperture): LIDT increased 1.5x for 1030 nm ($F = 0.28 - 0.31 \text{ J/cm}^2$ to $F = 0.38 - 0.47 \text{ J/cm}^2$) and 2.7x for 515 nm radiation (from $F = 0.07 - 0.08 \text{ J/cm}^2$ to $F = 0.19 - 0.21 \text{ J/cm}^2$).

The observed increase of LIDT in CA structures could potentially be attributed to improved thermal transfer and enhanced chemical bonding mechanisms.

Author Contributions: Conceptualization, D.G. and M.M.; methodology, D.G.; software, R.Z.; validation, K.G.; formal analysis, D.G., K.G., G.B. and M.M.; investigation, R.Z.; resources, D.G. and M.M.; writing—original draft preparation, D.G.; writing—review and editing, K.G., G.B. and M.M.; visualization, R.Z.; supervision, D.G. and M.M.; project administration, M.M.; funding acquisition, M.M. All authors have read and agreed to the published version of the manuscript.

Funding: This research received funding from EU Horizon 2020, Research and Innovation program LASERLAB-EUROPE JRA Project No. 871124.

Data Availability Statement: The data presented in this study are available on request from the corresponding author.

Acknowledgments: We acknowledge Maria Farsari and Vasileia Melissinaki for kindly providing the authors with the SZ2080TM (IESL-FORTH, Heraklion, Greece) hybrid organic–inorganic materials for performing the described experiments. We thank Andrius Melninkaitis (Vilnius University, Faculty of Physics, Laser Research Center/LIDARIS Ltd.) for consultation regarding LIDT.

Conflicts of Interest: The authors declare no conflict of interest.

Abbreviations

The following abbreviations are used in this manuscript:

LIDT	Laser-Induced Damage Threshold
LDW	Laser Direct Writing
S-on-1	Series-on-One
PI	Photo-Initiator
CA	Calcinated
NCA	Non-Calcinated
SEM	Scanning Electron Microscope

References

1. Gonzalez-Hernandez, D.; Varapnickas, S.; Merkininkaitė, G.; Čiburys, A.; Gailevičius, D.; Šakirzanovas, S.; Juodkasis, S.; Malinauskas, M. Laser 3D Printing of Inorganic Free-Form Micro-Optics. *Photonics* **2021**, *8*, 577.
2. Wang, H.; Zhang, W.; Ladika, D.; Yu, H.; Gailevičius, D.; Wang, H.; Pan, C.; Nair, P.N.; Ke, Y.; Mori, T.; et al. Two-photon polymerization lithography for optics and Photonics: Fundamentals, materials, technologies, and applications. *Advanced Functional Materials* **2023**, p. 2214211. doi:10.1002/adfm.202214211.
3. Wu, D.; Chen, Q.D.; Niu, L.G.; Jiao, J.; Xia, H.; Song, J.F.; Sun, H.B. 100% Fill-Factor Aspheric Microlens Arrays (AMLA) With Sub-20-nm Precision. *IEEE Photonics Technology Letters* **2009**, *21*, 1535–1537. doi:10.1109/LPT.2009.2029346.
4. Asadollahbaik, A.; Thiele, S.; Weber, K.; Kumar, A.; Drozella, J.; Sterl, F.; Herkommer, A.M.; Giessen, H.; Fick, J. Highly Efficient Dual-Fiber Optical Trapping with 3D Printed Diffractive Fresnel Lenses. *ACS Photonics* **2020**, *7*, 88–97. doi:10.1021/acsp Photonics.9b01024.
5. Sandford O'Neill, J.; Salter, P.; Zhao, Z.; Chen, B.; Dagainawalla, H.; Booth, M.J.; Elston, S.J.; Morris, S.M. 3D Switchable Diffractive Optical Elements Fabricated with Two-Photon Polymerization. *Advanced Optical Materials* **2022**, *10*, 2102446. doi:10.1002/adom.202102446.

6. Mu, H.; Smith, D.; Katkus, T.; Gailevičius, D.; Malinauskas, M.; Nishijima, Y.; Stoddart, P.R.; Ruan, D.; Ryu, M.; Morikawa, J.; et al.. Polarisation control in arrays of Microlenses and gratings: Performance in visible–IR spectral ranges. *Micromachines* **2023**, *14*, 798. doi:10.3390/mi14040798.
7. Faniayeu, I.; Khakhomov, S.; Semchenko, I.; Mizeikis, V. Highly transparent twist polarizer metasurface. *Applied Physics Letters* **2017**, *111*, 1–5. doi:10.1063/1.4994777.
8. Žukauskas, A.; Malinauskas, M.; Brasselet, E. Monolithic generators of pseudo-nondiffracting optical vortex beams at the microscale. *Applied Physics Letters* **2013**. doi:10.1063/1.4828662.
9. Thiele, S.; Arzenbacher, K.; Gissibl, T.; Giessen, H.; Herkommer, A.M. 3D-printed eagle eye: Compound microlens system for foveated imaging. *Science Advances* **2017**, *3*. doi:10.1126/sciadv.1602655.
10. Marini, M.; Nardini, A.; Martínez Vázquez, R.; Conci, C.; Bouzin, M.; Collini, M.; Osellame, R.; Cerullo, G.; Kariman, B.S.; Farsari, M.; et al.. Microlenses fabricated by two-photon laser polymerization for cell imaging with non-linear excitation microscopy. *Advanced Functional Materials* **2023**, p. 2213926. doi:10.1002/adfm.202213926.
11. Galvanauskas, K.; Astrauskyte, D.; Balcas, G.; Gailevičius, D.; Grineviciute, L.; Malinauskas, M. High-transparency 3D micro-optics of hybrid-polymer SZ2080™ made via Ultrafast Laser Nanolithography and atomic layer deposition **2023**. doi:10.1364/opticaopen.22302655.v1.
12. Siegle, L.; Ristok, S.; Giessen, H. Complex aspherical singlet and Doublet Microoptics by Grayscale 3D printing. *Optics Express* **2023**, *31*, 4179. doi:10.1364/oe.480472.
13. Gonzalez-Hernandez, D.; Sanchez-Padilla, B.; Gailevicius, D.; Chandran Thodika, S.; Brasselet, E.; Malinauskas, M. Single-step 3D printing of micro-optics with adjustable refractiveindex by ultrafast laser nanolithography. *Advanced Optical Materials (In Press)* **2023**, p. 2300258. doi:10.1002/adom.202300258.
14. Gopinath, S.; Angamuthu, P.P.; Kahro, T.; Bleahu, A.; Arockiaraj, F.G.; Smith, D.; Ng, S.H.; Juodkazis, S.; Kukli, K.; Tamm, A.; et al.. Implementation of a large-area diffractive lens using multiple sub-aperture diffractive lenses and computational reconstruction. *Photonics* **2022**, *10*, 3. doi:10.3390/photonics10010003.
15. LaFratta, C.N.; Simoska, O.; Pelse, I.; Weng, S.; Ingram, M. A convenient direct laser writing system for the creation of Microfluidic Masters. *Microfluidics and Nanofluidics* **2015**, *19*, 419–426. doi:10.1007/s10404-015-1574-4.
16. Hu, Y.; Miles, B.T.; Ho, Y.L.D.; Taverne, M.P.; Chen, L.; Gersen, H.; Rarity, J.G.; Faul, C.F. Toward direct laser writing of actively tuneable 3D photonic crystals. *Advanced Optical Materials* **2016**, *5*, 1600458. doi:10.1002/adom.201600458.
17. Fischer, J.; Wegener, M. Three-dimensional optical laser lithography beyond the diffraction limit. *Laser and Photonics Reviews* **2012**, *7*, 22–44. doi:10.1002/lpor.201100046.
18. Vyatskikh, A.; Ng, R.C.; Edwards, B.; Briggs, R.M.; Greer, J.R. Additive manufacturing of high-refractive-index, nanoarchitected titanium dioxide for 3D dielectric photonic crystals. *Nano Letters* **2020**, *20*, 3513–3520. doi:10.1021/acs.nanolett.0c00454.
19. Hong, Z.; Ye, P.; Loy, D.A.; Liang, R. High-precision printing of complex glass imaging optics with precondensed liquid silica resin. *Advanced Science* **2022**, *9*, 2105595. doi:10.1002/advs.202105595.
20. Hong, Z.; Ye, P.; Loy, D.A.; Liang, R. Three-dimensional printing of glass micro-optics. *Optica* **2021**, *8*, 904. doi:10.1364/optica.422955.
21. ISO 21254-2:2011 Lasers and laser-related equipment – Test methods for laser-induced damage threshold. *Standard, International Organization for Standardization, Geneva, Switzerland* **2011**.
22. Stankova, N.; Atanasov, P.; Nikov, R.; Nikov, R.; Nedyalkov, N.; Stoyanchoy, T.; Fukata, N.; Kolev, K.; Valova, E.; Georgieva, J.; Armanyanov, S. Optical properties of polydimethylsiloxane (PDMS) during nanosecond laser processing. *Applied Surface Science* **2016**, *374*, 96–103. doi:10.1016/j.apsusc.2015.10.016.
23. Saha, S.K.; Divin, C.; Cuadra, J.A.; Panas, R.M. Effect of proximity of features on the damage threshold during submicron additive manufacturing via two-photon polymerization. *Journal of Micro and Nano-Manufacturing* **2017**, *5*. doi:10.1115/1.4036445.
24. Žukauskas, A.; Batavičiūtė, G.; Ščiuka, M.; Jukna, T.; Melninkaitis, A.; Malinauskas, M. Characterization of photopolymers used in laser 3D micro/nanolithography by means of laser-induced damage threshold (LIDT). *Optical Materials Express* **2014**, *4*, 1601. doi:10.1364/OME.4.001601.
25. Žukauskas, A.; Batavičiūtė, G.; Ščiuka, M.; Balevičius, Z.; Melninkaitis, A.; Malinauskas, M. Effect of the photoinitiator presence and exposure conditions on laser-induced damage threshold of ORMOSIL (SZ2080). *Optical Materials* **2015**, *39*, 224–231. doi:10.1016/j.optmat.2014.11.031.

26. Gallais, L.; Commandré, M. Laser-induced damage thresholds of bulk and coating optical materials at 1030 nm, 500 fs. *Applied Optics* **2014**, *53*, A186. doi:10.1364/AO.53.00A186.
27. Butkutė, A.; Čekanavičius, L.; Rimšelis, G.; Gailevičius, D.; Mizeikis, V.; Melninkaitis, A.; Baldacchini, T.; Jonušauskas, L.; Malinauskas, M. Optical damage thresholds of microstructures made by laser three-dimensional nanolithography. *Opt. Lett.*, *45*, 13–16.
28. Simakov, E.; Gilbertson, R.; Herman, M.; Pilania, G.; Shchegolkov, D.; Walker, E.; England, R.; Wootton, K. Possibilities for Fabricating Polymer Dielectric Laser Accelerator Structures with Additive Manufacturing. *Ipac 2018* **2018**, pp. 9–12. doi:10.18429/JACoW-IPAC2018-THPML011.
29. Samsonas, D.; Skliutas, E.; Ciburyš, A.; Kontenis, L.; Gailevičius, D.; Berzinš, J.; Narbutis, D.; Jukna, V.; Vengris, M.; Juodkazis, S.; Malinauskas, M. 3D nanopolymerization and damage threshold dependence on laser wavelength and pulse duration. *Nanophotonics* **2023**. doi:10.1515/nanoph-2022-0629.
30. Kabouraki, E.; Melissinaki, V.; Yadav, A.; Melninkaitis, A.; Tourlouki, K.; Tachtsidis, T.; Kehagias, N.; Barmparis, G.D.; Papazoglou, D.G.; Rafailov, E.; Farsari, M. High laser induced damage threshold photoresists for nano-imprint and 3D multi-photon lithography. *Nanophotonics* **2021**, *10*, 3759–3768. doi:10.1515/nanoph-2021-0263.
31. Merkininkaitė, G.; Aleksandravičius, E.; Malinauskas, M.; Gailevičius, D.; Šakirzanovas, S. Laser additive manufacturing of SiZrO₂ tunable crystalline phase 3D nanostructures. *Opto-Electr. Adv.* **2022**, *5*, 210077.
32. Ovsianikov, A.; Viertl, J.; Chichkov, B.; Oubaha, M.; MacCraith, B.; Sakellari, I.; Giakoumaki, A.; Gray, D.; Vamvakaki, M.; Farsari, M.; Fotakis, C. Ultra-Low Shrinkage Hybrid Photosensitive Material for Two-Photon Polymerization Microfabrication. *ACS Nano* **2008**, *2*, 2257–2262. doi:10.1021/nn800451w.
33. Merkinaite, G.; Gailevicius, D.; Staisiunas, L.; Ezerskyte, E.; Vargalis, R.; Malinauskas, M.; Sakirzanovas, S. Additive Manufacturing of Extremely Hard SiOC Ceramic 3DMicro-Structures. *Submitted* **2023**.
34. Butkus, A.; Skliutas, E.; Gailevičius, D.; Malinauskas, M. Femtosecond-laser direct writing 3D micro/nano-lithography using VIS-light oscillator. *Journal of Central South University* **2022**, *29*, 3270–3276. doi:10.1007/s11771-022-5153-z.
35. Garrison, B.J.; Srinivasan, R. Laser ablation of organic polymers: Microscopic models for photochemical and thermal processes. *Journal of Applied Physics* **1985**, *57*, 2909–2914. doi:10.1063/1.335230.
36. Jonusauskas, L.; Gailevicius, D.; Mikoliunaite, L.; Sakalauskas, D.; Šakirzanovas, S.; Juodkazis, S.; Malinauskas, M. Optically clear and resilient free-form u-optics 3D-printed via Ultrafast Laser Lithography. *Materials* **2017**, *10*, 12. doi:10.3390/ma10010012.
37. Vlassov, S.; Oras, S.; Timusk, M.; Zadin, V.; Tiirats, T.; Sosnin, I.M.; Löhms, R.; Linarts, A.; Kyritsakis, A.; Dorogin, L.M.; et al.. Thermal, mechanical, and acoustic properties of polydimethylsiloxane filled with hollow glass microspheres. *Materials* **2022**, *15*, 1652. doi:10.3390/ma15051652.
38. OrmoComp®.
39. Chang, C.H.; Lin, C.Y.; Chang, C.H.; Liu, F.H.; Huang, Y.T.; Liao, Y.S. Enhanced biomedical applicability of zro2-sio2 ceramic composites in 3D printed bone scaffolds. *Scientific Reports* **2022**, *12*. doi:10.1038/s41598-022-10731-w.
40. Barkaline, V.V.; Nelayev, V.V.; Chashinski, A.S. SiO₂ on CNT: Molecular dynamics simulation. *SPIE Proceedings* **2006**. doi:10.1117/12.676302.
41. Smalakys, L.; Melninkaitis, A. Predicting lifetime of optical components with bayesian inference. *Optics Express* **2021**, *29*, 903. doi:10.1364/oe.410844.
42. Ward, J.M.; Yang, Y.; Nic Chormaic, S. Glass-on-glass fabrication of bottle-shaped tunable microlasers and their applications. *Scientific Reports* **2016**, *6*. doi:10.1038/srep25152.
43. Balcas, G.; Malinauskas, F.; Maria, G.; Juodkazis, S. Fabrication of glass-ceramic 3D micro-optics by combining laser lithography and calcination. *Advanced Functional Materials (Accepted)* **2023**.

Disclaimer/Publisher's Note: The statements, opinions and data contained in all publications are solely those of the individual author(s) and contributor(s) and not of MDPI and/or the editor(s). MDPI and/or the editor(s) disclaim responsibility for any injury to people or property resulting from any ideas, methods, instructions or products referred to in the content.